

## Computer Aided Visual Inspection of Aircraft Surfaces

### Rafia Mumtaz

*School of Electrical Engineering and Computer Science  
National University of Sciences and Technology  
Sector H-12, Islamabad, Pakistan*

*rafia.mumtaz@seecs.edu.pk*

### Mustafa Mumtaz

*College of Aeronautical Engineering  
National University of Sciences and Technology  
Sector H-12, Islamabad, Pakistan*

*mustafa672@ieee.org*

### Atif Bin Mansoor

*College of Aeronautical Engineering  
National University of Sciences and Technology  
Sector H-12, Islamabad, Pakistan*

*atif-cae@nust.edu.pk*

### Hassan Masood

*College of Aeronautical Engineering  
National University of Sciences and Technology  
Sector H-12, Islamabad, Pakistan*

*hassan13204@yahoo.com*

---

### Abstract

Non Destructive Inspections (NDI) plays a vital role in aircraft industry as it determines the structural integrity of aircraft surface and material characterization. The existing NDI methods are time consuming, we propose a new NDI approach using Digital Image Processing that has the potential to substantially decrease the inspection time. Automatic Marking of cracks have been achieved through application of Thresholding, Gabor Filter and Non Subsampled Contourlet transform. For a novel method of NDI, the aircraft imagery is analyzed by three methods i.e Neural Networks, Contourlet Transform (CT) and Discrete Cosine Transform (DCT). With the help of Contourlet Transform the two dimensional (2-D) spectrum is divided into fine slices, using iterated directional filterbanks. Next, directional energy components for each block of the decomposed subband outputs are computed. These energy values are used to distinguish between the crack and scratch images using the Dot Product classifier. In next approach, the aircraft imagery is decomposed into high and low frequency components using DCT and the first order moment is determined to form feature vectors. A correlation based approach is then used for distinction between crack and scratch surfaces. A comparative examination between the two techniques on a database of crack and scratch images revealed that texture analysis using the combined transform based approach gave the best results by giving an accuracy of 96.6% for the identification of crack surfaces and 98.3% for scratch surfaces.

**Keywords:** Computer Vision, Gabor Filter, Contourlet Transform, Non Subsampled Contourlet Transform, Discrete Cosine Transform, Neural Networks.

---

## 1. INTRODUCTION

Vision is the most advanced of our senses, so the concept of keeping or storing one of these senses i.e. the visual sense, seems interesting to all the human beings. Today images are being used in almost all applications of daily day life and research. Satellite and space imagery, industrial radiographs, radars and photoreconnaissance, infrared studies, mapping, pollution analysis etc use images as a basic tool for their study. With the advancement in other fields of study and research, image processing developed itself from optical (analog) processing to DIGITAL IMAGE PROCESSING (DIP). Visual inspection of aircraft is widely used for ensuring

structural integrity of surface and its substructures. Visual inspector examines an aircraft for defects such as cracks, corrosion, damaged rivets, bird hit, lightning strike etc [1]. The inspection may suffer due to many reasons like competence level of inspector, lack of interest boredom or delicate nature of defect etc. Enhanced visual inspection could allow the inspector to safely, quickly and accurately perform the necessary visual inspection.

Non Destructive Inspection (NDI) techniques are used in aerospace industry for analyzing the aircraft surface and sub-surface defects. These techniques along with the visible cracks detect the microscopic cracks too. As stated in [2], the importance of aircraft surface inspections lies from the fact that a typical heavy inspection of a commercial aircraft is 90% visual and 10% NDI. Visual inspection helps in isolating the surface of the aircraft that may suffer from any failure. Commonly employed NDI techniques are Dye Penetrant Method, Fluorescent Penetrant Inspection, Magnetic Particle Inspection (MPI), Eddy Current Losses, Radiography, and Ultrasonic Inspection. These NDI techniques suffer from more down time and require large and costly setups. Robotics Institute of Carnegie Mellon University has carried out a research in development of a robot known as Crown Inspection Mobile Platform (CIMP) [2], [3]. This robot is capable of moving over the aircraft body and transmitting live stereoscopic imagery of the aircraft to the control center. The control center applies image enhancement and understanding algorithm to highlight areas of cracks and scratches. [4] made a similar research by acquiring aircraft images by a robot and subsequently processing them by Neural Networks. Training was performed by giving different images of multiple fasteners used in a modern aircraft. The technique resulted in differentiating healthy and crack areas of the aircraft surface.

This research is aimed to investigate various image processing algorithms to develop a cost effective and computationally efficient computer aided visual inspection of aircraft surface. The project involves real data collection by identifying and photographing crack susceptible areas of aircraft. In Section 2 Suggestions are formalized for inclusion of surface imaging in existing periodic inspections. Automatic marking of cracks is investigated through different methods like thresholding techniques of Otsu and Entropy, Gabor Filter for texture analysis, Nonsubsampled Contourlet transform and Neural Network as described in Section 3. Adaptive models have been optimized to address random illumination variations. A new visual method is devised to differentiate between crack and scratch other than the existing NDI techniques. Methods like Neural Network classifier, Discrete Cosine transform in collaboration with Dot Product classifier and energy calculations via Contourlet transform are applied in order to minimize False Alarm Rate. This method is elaborated in Section 4. Chapter is concluded in Section 5.

## **2. SUGGESTED SURFACE IMAGING**

In today's aviation industry weekly and periodic inspection is carried out in accordance with predefined manuals and work cards. These work cards provide the requirements of the applicable aircraft scheduled inspection and maintenance requirements. The manual provides a checklist form and is used as a guide in performing the inspection to ensure that no item is overlooked. The inspection requirements are tested in such a manner as to establish which equipment is to be inspected, when it is to be inspected, and what conditions are to be sought. In scope, the requirements are designed to direct the attention of maintenance personnel to components and areas where defects are suspected to exist as a result of usage under normal operating conditions. They are not intended to provide coverage for normal routine cleaning, washing, etc nor are they designed to lead to the detection of isolated discrepancies that are the result of carelessness or poor maintenance practices.

A new criteria is defined to carry out periodic inspection that is performed through imaging which will have the benefit of better record keeping and trend analysis of aircrafts. Various areas of aircraft that are prone to cracks were identified and were photographed weekly. The identified surfaces prone to cracks were photographed weekly. Suggested scale and angle were defined and maintained while photographing.

Before explaining the criteria it is necessary to mention here that illumination cannot be controlled while taking the photographs outside. Illumination variance is not only due to climatic change but also with time due to changing position of sun. Therefore it is highly recommended that photography should be carried out in an indoor environment like a hanger where the image quality is less prone to be degraded, moreover the illumination variance though still there; can be neglected safely.

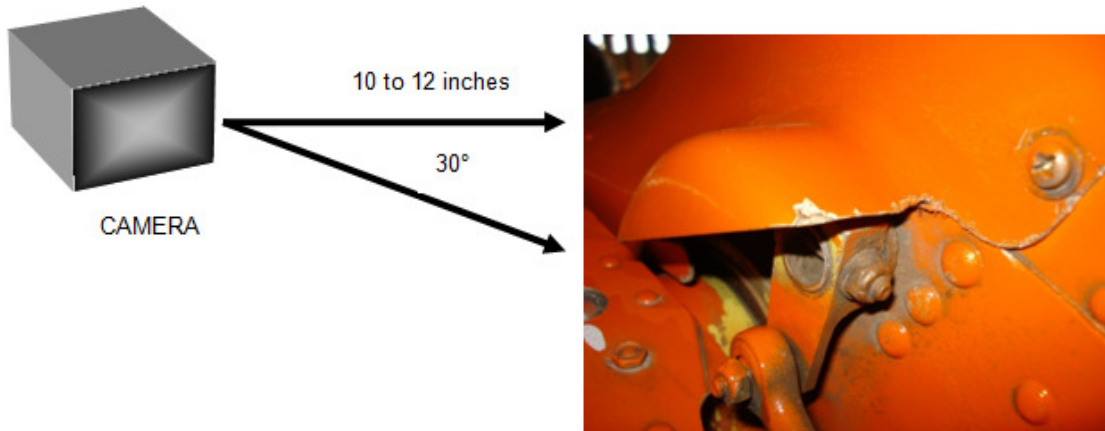


**FIGURE 1:** Elevator Surface

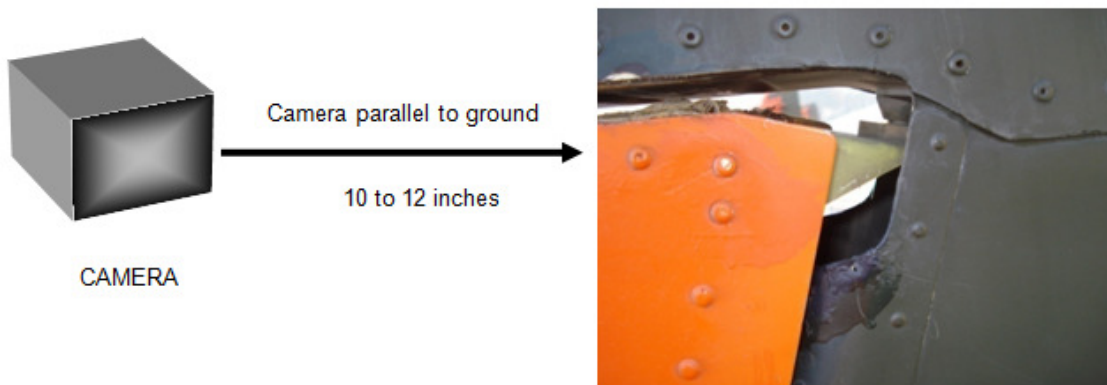


**FIGURE 2:** Rudder Surface

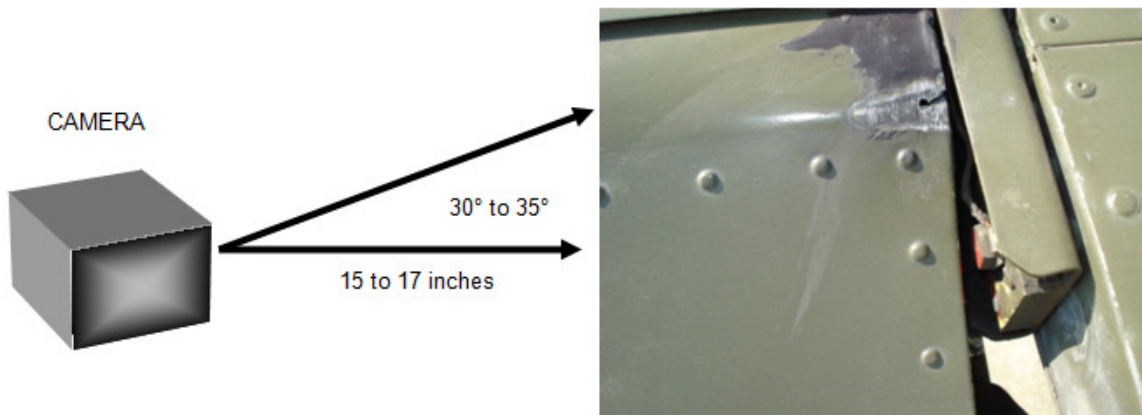


**FIGURE 3:** Flap Surface

These criteria can be demonstrated by showing different images of aircraft surfaces prone to stress during flight and subsequently generates surface cracks. Figure 1 shows how an aircraft elevator is photographed with suggested angle and distance. Figure 2 shows rudder surface while Figure 3 shows the flap surface. On similar basis photography methods are devised and formulated for wing root, tail cone, engine hot and cold flaps, engine jet pipe liners and nose cone surfaces.

### **3. AUTOMATIC MARKING OF CRACKS**

One of the main task in aiding visual inspection of aircraft is to automatically mark the cracked area of aircraft surface. The automatic marking of marks helps the user to instantaneous get the information of cracked surface from the surface imaging data set area but also to find out which orientation it is following. It helps the inspector to carry out inspection which raises safety issues for the inspector, is time consuming, and suffers at times from being ineffective due to inspector fatigue or boredom [1]. Automatic marking could allow the inspector to safely, quickly and accurately perform the necessary visual inspection.

Automatic marking of cracks have been performed through various techniques. These methods are based on thresholding based, texture based, transform based and classifier based models. The applications of various techniques were due to nature and quality of images which vary basically because of illumination.

#### **3.1 Thresholding Techniques**

Thresholding is an important technique for image segmentation that tries to identify and extract a target from its background on the basis of the distribution of gray levels or texture in image objects. Most Thresholding techniques are based on the statistics of the one-dimensional (1D) histogram of gray levels and on the two dimensional (2D) co-occurrence matrix of an image [5], [6], [7]. Automatic marking of cracks is dramatically affected by changes in the illumination conditions of image captured. In general the variation between images of different cracks captured in the same conditions is smaller than that of the same crack taken in a variety of environments. Two methods are used for thresholding images. These are Otsu Method of Thresholding and Entropy Method of Thresholding.

##### **3.1.1 Otsu Method of Thresholding**

Nobuyuki Otsu in 1979 proposed an algorithm for automatic threshold selection from a histogram of image. The algorithm is based on discriminant analysis and uses the zeroth- and the first order cumulative moments of the histogram for calculating the value of the thresholding level. This is an unsupervised method of thresholding. An optimal threshold is selected by the discriminant criterion, namely, so as to maximize the separability of the resultant classes in gray levels [8]. After thresholding the image, the binary image obtained has black background with crack information in white pixels. The coordinates of white pixels were then extracted and were plotted on the original image with a pseudo color as shown in Figure 4.

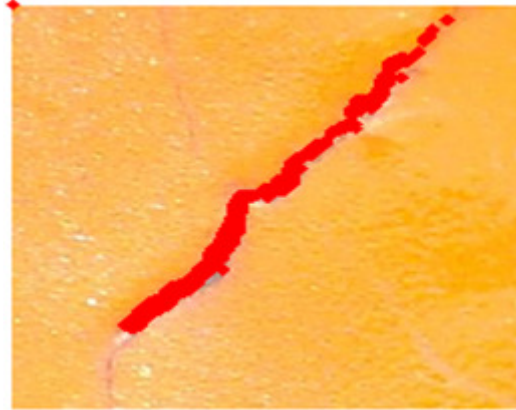


**FIGURE 4:** Marking of Crack by Otsu Method of Thresholding

### 3.1.2 Entropy Method of Thresholding

The entropy-based techniques have proven to be successful and reasonably robust [9], however they suffer various limitations and are sensitive to noise. These techniques rely on the total entropy of both the object and background regions to find the appropriate threshold. Some of these methods also make use of the pixels' spatial information. The method is very similar to Otsu's method. Rather than maximizing the inter-class variance, it maximizes the inter-class entropy. Entropy is a measure of the uncertainty of an event taking place. It can be calculated as:

$$S = -\sum (p) \times \log (p) \quad (1)$$

so it is very straightforward to do using the histogram data.  $P$  is the probability of a pixel grayscale value in the image, and  $\sum$  is the Greek capital sigma. It is customary to use  $\log$  in base 2. Figure 5 is an example of entropy principle of thresholding.

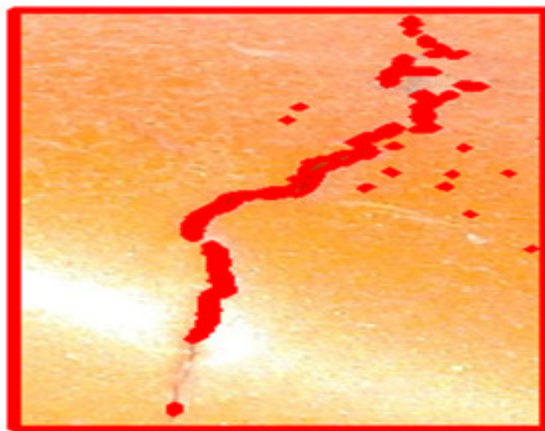


**FIGURE 4:** Marking of Crack by Entropy Method of Thresholding

### 3.2 Texture Analysis

The human's capability to distinguish perceptually different textures is difficult to reproduce using machine vision due to the variety of textural patterns and illumination conditions. Textures are modeled as a pattern dominated by a narrow band of spatial frequencies and orientations. Textures are used extensively by the human visual system to perform tasks such as the segmentation of scenes into distinct objects and the analysis of surface geometries. Each texture can thus be thought of as containing a narrow range of frequency and orientation components. By filtering the image with band-pass filter tuned to the dominant frequency and orientation component of the textures, it is possible to locate each texture. Therefore Gabor filter was the

best option in this case because Gabor filters are band-pass filters with tune able center frequency, orientation and bandwidth, properly tuned Gabor filters react strongly to specific textures and weakly to all others [10].

### 3.2.1 Gabor Filter

Gabor filters are a traditional choice for obtaining ontourle frequency information. They offer the best simultaneous localization of spatial and frequency information. [11] suggests that natural images are better coded by filters that have Gaussian transfer functions when viewed on the logarithmic frequency scale. (Gabor functions have Gaussian transfer functions when viewed on the linear frequency scale). On the linear frequency scale the log-Gabor function has a transfer function as shown in equation 2.

$$G(w) = e^{(-\log(w/w_0)^2) / (2 (\log(k/w_0))^2)} \tag{2}$$

where  $w_0$  is the filter's centre frequency. To obtain constant shape ratio filters the term  $k/w_0$  must also be held constant for varying  $w_0$ . In the frequency domain the even symmetric filter is represented by two real-valued log-Gaussian bumps symmetrically placed on each side of the origin. The odd-symmetric filter is represented by two imaginary valued log-Gaussian bumps anti-symmetrically placed on each side of the origin. The final transfer function is obtained by adding both even and odd transfer functions. Cracks have different orientations and have a set range of frequency. Therefore Gabor filter can give good results after finding orientation through extensive testing. But for every image we have to set the frequency and orientation information separately and that cannot be used by other images. Let us have a look at this image in Figure 4 where Gabor filter gave a good result in marking the crack when set to specific frequency and orientation In Figure 5, when same frequency and orientation was applied, the frequency of Gabor filter does not created any problem but only a mismatch in orientation created abnormal behavior. The crack which has the orientation similar to the crack in Figure 4 was detected rest was washed out.



**FIGURE 4:** Marking of Crack by Gabor Filter

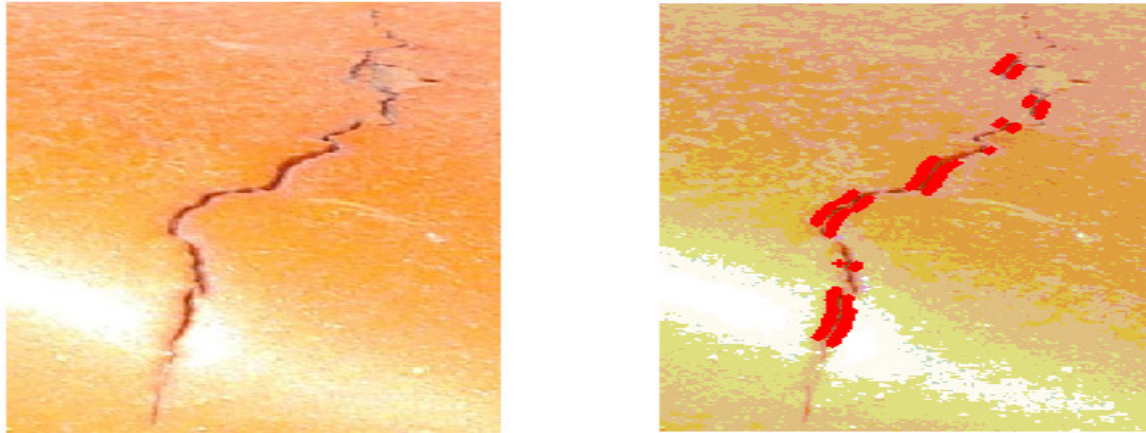


**FIGURE 5:** Marking of Crack by Gabor Filter

### 3.3 Transform Domain

The frequency spectrum of a signal is basically the frequency components (spectral components) of that signal. The frequency spectrum of a signal shows what frequencies exist in the signal [12]. Intuitively, it is known that the frequency is something to do with the change in rate of something. If something changes rapidly, it is of high frequency, where as if this variable does not change rapidly, i.e., it changes smoothly, it is of low frequency. If this variable does not change at all, it has zero frequency, or no frequency.

Often times, the information that cannot be readily seen in the time-domain can be seen in the frequency domain. By looking at the advantage of frequency information several transforms have been proposed for image signals that have incorporated directionality and multiresolution and hence, could more efficiently capture edges in natural images. Many transform like Wavelet, Contourlet and Nonsampled Contourlet are there to provide multiresolution and multidirectional information and each of them of them have their own limitations. In case of Wavelet which is a more general transform have three major flaws. It is shift sensitive because it implies that DWT coefficients fail to distinguish between input- signal shifts [13]. It lacks directional information as natural images contain number of smooth regions and edges with random orientations which affects the optimal representation of natural images. Finally it has absence of phase information which is sensitive to our visual system. Owing to the geometric information, the Contourlet transform achieves better results than discrete wavelet transform in image analysis applications such as denoising and texture retrieval. It is proposed by Minh Do and Martin Vetterli [14] and provides sparse representation at both spatial and directional resolutions. Contourlet transform uses a structure similar to that of curvelets [15]. The pyramidal filter bank structure of the Contourlet transform has very little redundancy, which is important for compression applications. However, Shift sensitivity is an undesirable property because it implies that the transform coefficients fail to distinguish between input- signal shifts. Shift-invariance is desirable in image analysis applications such as edge detection, contour characterization, and image enhancement.

#### 3.3.1 Non Subsampled Contourlet Transform

A shift-invariant version of the Contourlet transform is proposed which is built upon iterated non sub sampled filter banks to obtain a shift-invariant directional multiresolution image representation [16]. Shift invariance is a desirable property in many image processing applications [17]. Due to no down and up sampling NSCT has more redundancy but by allowing redundancy, it is possible to enrich the set of basic functions so that the representation is more efficient in capturing some signal behavior. Figure 6 depicts two channel non subsampled pyramid and directional filter banks used in non sub-sampled contourlet transform. Figure 7 shows how an input image is split into high pass subbands and low pass subbands by a non subsampled pyramid and then a directional filterbank decomposes a high subband into several directional subbands.

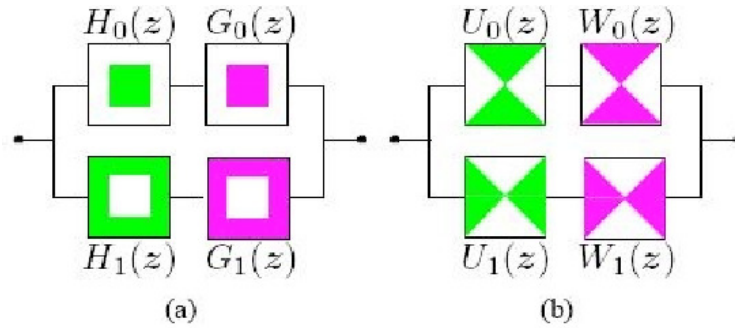


**FIGURE 6:** (a) Non Subsampled Pyramid (b) Non Subsampled Directional Filter Bank [16]

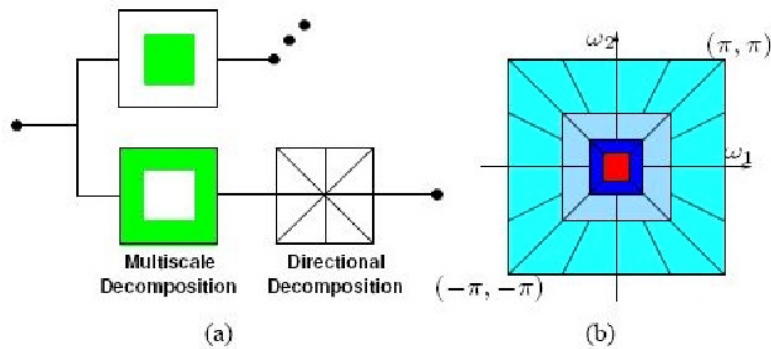


**FIGURE 7:** The nonsubsampled contourlet transform: (a) Block diagram. First, a nonsubsampled pyramid split the input into a lowpass subband and a highpass subband. Then a nonsubsampled DFB decomposes the highpass subband into several directional subbands. The scheme is iterated repeatedly on the lowpass subband. (b) Resulting frequency division, where the number of directions is increased with frequency [16]. The crack image was decomposed to 3 levels with 8 different directional sub-band. The 3rd level decomposition with 8 different directional sub-band was extracted which contains crack information in different direction. The selected sub-band were added which contains maximum crack information through an automatic thresholding technique devised separately. Automatic thresholding was devised in such a manner that it counts average amount of white pixels in the sub-band which are representing crack and if the white pixels are less than a specified value, which was calculated through extensive testing, they are discarded because they corresponds to noise. Then a union operation is applied between added coefficients of all the sub-bands and selected added coefficients.

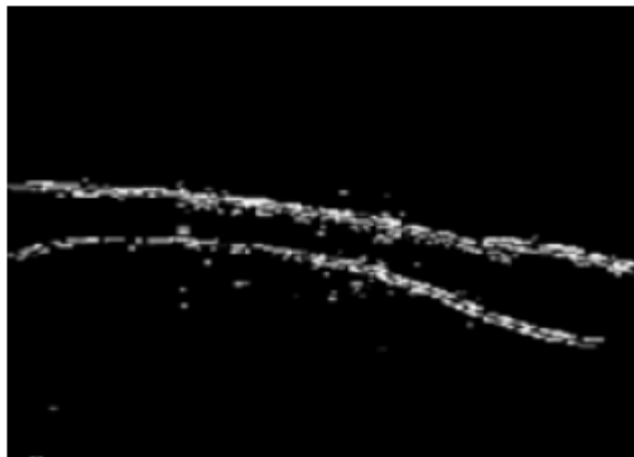


**FIGURE 8:** Marking of Crack by NSCT

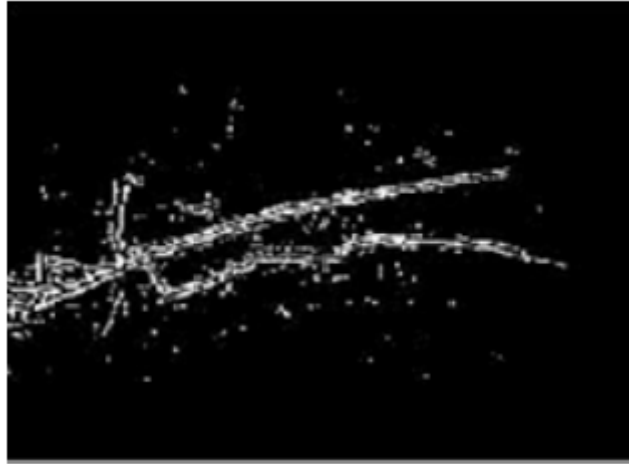


**FIGURE 9:** Marking of Crack by NSCT

From Figure 8 and Figure 9 it shows that Nonsubsampled Contourlet transform identified the crack in a right fashion and crack was not washed out at any location. NSCT gave finer results for automatically mark the cracked area of aircraft surface.

#### **4. DIFFERENTIATING CRACK AND SCRATCH**

To address so as how to differentiate between crack and scratch is quite challenging and obviously a difficult task. One must be careful not to evaluate on the basis of how this surface looks like because when the matter comes for aircraft there is no way to take any chance otherwise results could be hazardous and may lead the aircraft to crash. Sometime a surface seems to be scratch, after testing verifies to be crack and vice versa.

In this section a new method of differentiating between crack and scratch is proposed which is totally different from the existing NDI (Non-Destructive Inspection) techniques used in Aviation Industry. The desired surface to be judged as crack or scratch is performed through image processing techniques. Machine vision is used to make a decision whether the input surface is a crack or scratch [18]. The existing methods use in Aviation industry are time consuming and requires a lot of time for maintenance which makes the aircraft to remain ground for a longer period but if the required image of the defected place is available then it will definitely reduce the maintenance time causing the aircraft utilization to its maximum limits.

Three methods have been used to differentiate between crack and scratch. They are (a) Application of Neural Network (b) Energy Calculation (c) Discrete Cosine Transform with Dot Product Classifier

##### **4.1 Application of Neural Network**

Artificial neural networks are made up of interconnecting artificial neurons (programming constructs that mimic the properties of biological neurons) [19]. Artificial neural networks may either be used to gain an understanding of biological neural networks, or for solving artificial intelligence problems without necessarily creating a model of a real biological system. A single neuron may be connected to many other neurons and the total number of neurons and connections in a network may be extensive. Commonly neural networks are adjusted, or trained, so that a particular input leads to a specific target output. There, the network is adjusted, based on a comparison of the output and the target, until the network output matches the target. A simple Neural Network is shown in Figure 10.

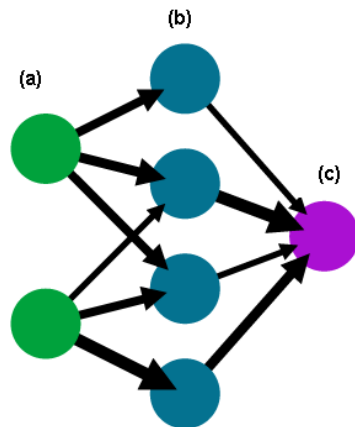


**FIGURE 10:** A simple Neural Network (a) Input Layer (b) Hidden Layer (c) Output Layer

#### 4.1.1 Proposed Algorithm

To train the network so as to differentiate whether the incoming image is a scratch or crack, 300 samples of crack and 300 samples of scratch were taken to train the network. The orientation and width of crack and scratch were random. The network was then trained accurately without any saturation. Training was improved by increasing the number of neurons which causes more distance between values so as to reduce overlapping regions, decreasing the Goal so as to minimize false alarm rate (FAR) and increasing number of Epochs which corresponds to number of iterations. Performance curve achieved for this network is shown in Figure 11. Cracks were given a weight of +1 while scratches were given a weight of -1. Training is said to be successful if performance curve touches the goal without any saturation.

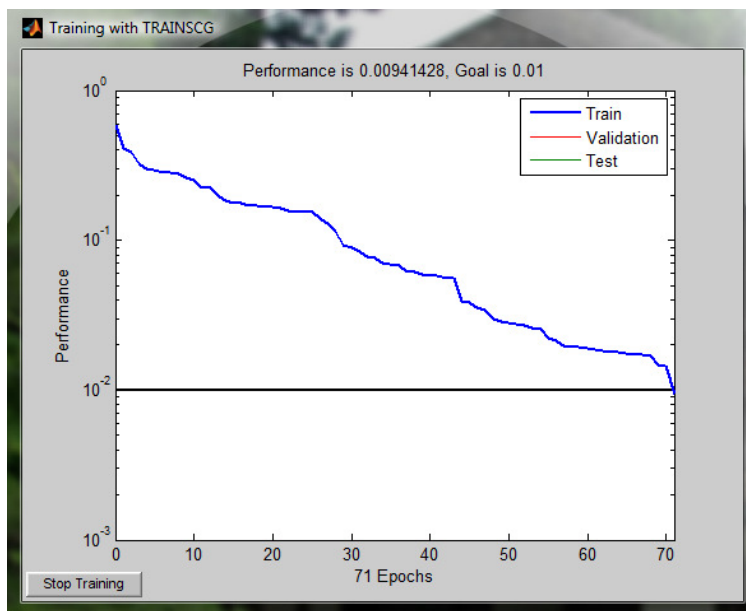


**FIGURE 11:** Performance Curve of Neural Network

#### 4.1.2 Testing and Evaluation

For detailed testing and evaluation of the algorithm another set of 300 cracks and 300 scratch images were taken to validate the method. The algorithm gave 19% FAR for crack and 11% for scratch. Although the FAR was quite high but the process of differentiating between crack and scratch via machine vision was a success.

#### 4.2 Energy Calculation

Another approach used to differentiate between crack and scratch was performed with the help of energy calculation. It was assumed that energy of crack should be higher than that of scratch therefore search to find an optimum threshold was necessary to distinguish both features. Energy method was performed through Contourlet Transform [20].

##### 4.2.1 Proposed Algorithm

The images are decomposed into sub-bands at four different resolution levels. At each resolution level 'k' the images are decomposed in  $2^n$  sub-bands where 'n' is the order of the directional filter. The highest resolution level (level 1) corresponds to the actual size of image i.e. 128 x 128. The next resolution level is determined by the expression  $2^{N-1}$  where N in this case is 7. This gives us an image of size 64 x 64 at level 2. Similarly the image is further reduced by subsampling at levels 3 and 4 and generating images of sizes 32 x 32 and 16 x 16 respectively. We have empirically chosen to apply a 5th order filter at resolution level 1 thus giving a total of 32 subbands. By applying a 4th order filter at resolution level 2, 16 subband outputs are obtained. Similarly resolution levels 3 and 4 gave 8 and 4 subbands respectively. Resultantly, 60 valued feature vector is calculated by finding the directional energies in respective sub-bands. Decomposition at three resolution levels is shown in Figure 12.

$E_{k\theta}$ , defined as the Energy value in directional sub-band  $S_{k\theta}$  at  $k^{th}$  resolution level is given by:

$$E_{k\theta} = \sum_{x,y} |F_{k\theta}(x,y) - \overline{F_{k\theta}}| \quad (3)$$

where  $\overline{F_{k\theta}}$  is the mean of pixel values of  $F_{k\theta}(x,y)$  in the sub-band  $S_{k\theta}$ .  $F_{k\theta}(x,y)$  is the contourlet coefficient value at position  $(x,y)$ . Additionally, the directional sub-bands vary from 0 to  $2^n - 1$ . The normalized energy value  $\overline{E_{k\theta}}$  of the subband  $\theta$  at  $k^{th}$  resolution level is defined as:

$$\overline{E_{k\theta}} = \frac{E_{k\theta}}{\sum_{\theta=0}^{2^n-1} E_{k\theta}} \quad (4)$$

Taking the constant  $F_{max}$  value equal to maximum intensity level of 255, the feature value  $F_{k\theta}$  is calculated as:

$$F_{k\theta} = F_{max} \times \overline{E_{k\theta}} \quad (5)$$

We have evaluated the performance of our proposed algorithm by using the Contourlet Toolbox available at [21]. We used PKVA (Ladder Filter) as the selected filter for our algorithm. Feature vectors are calculated for the images and are stored in a gallery.

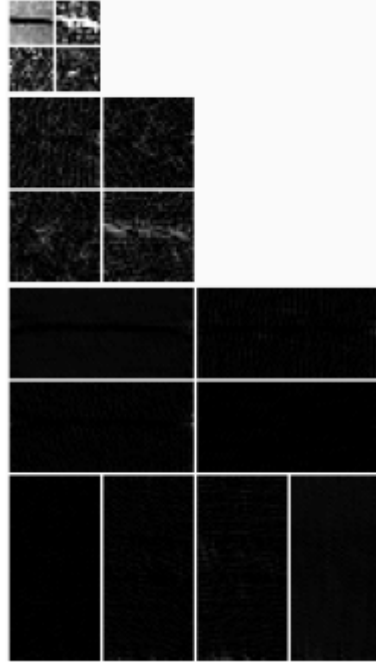


FIGURE 12: Sub band decomposition at three resolution levels

#### 4.2.2 Experimental Results

Proposed algorithm has been implemented in MATLAB on a 1.5 GB RAM, 1.67 GHz Intel Core Duo processor PC. The data set of 600 images of crack and 600 images of scratch were divided into two parts. Therefore, out of 600 images of crack and scratch each, 300 images were used for the purpose of training respectively. These training images were subjected to the Contourlet transform as described in the previous section and their feature vectors were stored separately. The rest 300 images of crack and 300 images of scratch were used for the purpose of validation. These test images were subjected to Contourlet Transform and their feature vectors were passed through the Dot Product Classifier with the feature vectors of training images. The dot product giving the highest result with the training images was finalized to give decision of the crack or scratch. It was observed that the directional energy components of the image of crack and scratch are highly overlapping resulting in classification errors as depicted in Figure 13. This method was able to identify 200 images of scratch and 225 images of crack out of 300 images of crack and scratch respectively.

#### 4.3 Discrete Cosine Transform

Discrete Cosine Transform packs image into its low frequency components [22]. DCT has many applications in the field of Image processing. It bears the property of de-correlation, energy compaction, separability which means that 1-D DCT can be applied to rows and then columns of an image. DCT has vast applications in the field of feature extraction and pattern recognition. Two dimensional DCT is defined as:

$$C(u, v) = a(u) a(v) \sum_{x=0}^{N-1} \sum_{y=0}^{N-1} f(x, y) \cos \frac{\pi(2x+1)u}{2N} \cos \frac{\pi(2y+1)v}{2N} \quad (6)$$

For  $u, v = 0, 1, 2, 3, \dots, N-1$  and  $a(u)$  and  $a(v)$  are defined as

$$a(u) = \begin{cases} \sqrt{\frac{1}{N}} \text{ for } u = 0 \\ \sqrt{\frac{2}{N}} \text{ for } u \neq 0 \end{cases} \quad (7)$$

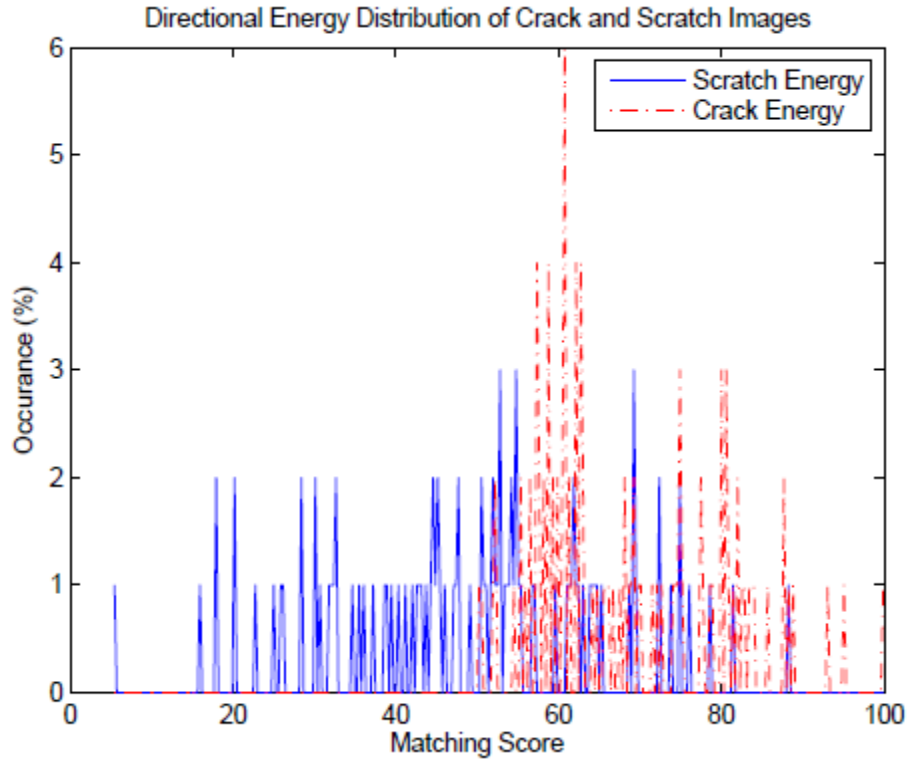


**FIGURE 13:** Directional Energy distribution of Sub bands

#### 4.3.1 Application of DCT

The images that were previously used for training the CT were utilized for feature extraction by the DCT. Each image of crack and scratch was decomposed into 100 segments each of size 10 X 10 pixels as shown in Figure 14.

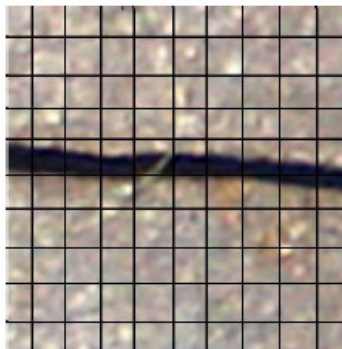


**FIGURE 14:** Division of Image into 100 pieces

The DCT of individual segment is calculated and values near or equal to zero are discarded. Standard deviations for the rest of the coefficient values were calculated. This procedure is applied to 100 segments of an image to generate a feature vector of 100 length.

#### 4.3.2 Experimental Results

The size of the database of the crack and scratch images for the purpose of training and validation remains same as that of Contourlet Transform. Each of the image of crack and scratch used for the purpose of training was passed through DCT as described in the previous section

and its feature vector was stored separately. Similarly the images used for evaluation were subjected to DCT and their feature vectors were passed through the Dot Product Classifier with the feature vectors of training images. The dot product with the highest result was finalized to give decision of the crack or scratch. The DCT was able to identify 285 images of crack and 292 images of scratch out of 300 images of crack and scratch respectively leading to an accuracy of 95% and 97.3% respectively.

**4.4 Combination of Transforms**

To further enhance our approach, the feature vectors obtained from both the transforms of the training images were concatenated and stored in a separate gallery. The images used for validation were first passed through the Contourlet Transform and Discrete Cosine Transform as described in previous sections and their concatenated feature vectors were subjected to the Dot product classifier with rest of the feature vectors of the training images. The dot product with the highest result was observed with the training images to finalize the decision of crack or scratch. This technique resulted in better identification result, giving a higher recognition rate i.e. 96.6% for the crack surfaces and 98.3% for the scratch surfaces. This method identifies 290 images of crack and 295 images of scratch out of 300 images of crack and scratch surfaces respectively. Table 1 summarizes the results for the three approaches.

Test	CT	DCT	Combination of Transforms
Crack Images Identified	225	285	290
Scratch Images Identified	200	292	295
Recognition Rate of Crack Images (%)	75	95	96.6
Recognition Rate of Scratch Images (%)	66.66	97.3	98.3

**TABLE 1:** Comparison of Three approaches on a database of 300 crack and 300 scratch aircraft surfaces

**5. CONCLUSION**

The methods described depict intelligent utilization of Digital Image Processing for specified application. The proposed computer aided techniques are not only power efficient but they also consume less amount of time for maintenance. The inspection through image processing does not have the element of fatigue or boredom. Enhancement of aircraft imagery helps the user to have a broader view of image that have been either degraded due to poor lighting conditions, blurriness or addition of noise. A new visual method is devised to differentiate between crack and scratch to supplement existing NDI techniques. The differentiation between crack and scratch can be improved by varying the parameters of Neural Network or by increasing the data set of images for training the Neural Network or DCT with Dot product classifier. The proposed technique was capable of differentiating crack and scratch with 96.6% accuracy for crack and 98.3% accuracy for scratch. Suggestion are included to have surface imaging in existing periodic inspection for better record keeping and trend analysis of aircrafts. Various critical areas of aircraft that are susceptible to cracks were identified and were photographed with suggested scale and angle. Surface imaging along with automatic marking of cracks helps in analyzing the stress and strain analysis of aircrafts thus identifying aircrafts which requires more maintenance time. These methods in general reduce maintenance time thus ensuring maximum utilization of aircraft for flying.

**6. REFERENCES**

[1] Gunatilake P., Siegel M., Jordan A., and Podnar G. Image Understanding Algorithms for Remote Visual Inspection of Aircraft Surfaces, In: Machine Vision Applications in Industrial inspection V, page numbers (2-13), 1997

[2] Siegel M. and Gunatilake P. Enhanced Remote Visual Inspection of Aircraft Skin, In: Proc. Intelligent NDE Sciences for Aging and Futuristic Aircraft Workshop, page numbers (101-112), 1997

- [3] Siegel M., Gunatilake P. and Podnar. Robotic assistants for Aircraft Inspectors, In: Proc. IEEE Instrumentation and Measurement Magazine, Vol 1, page numbers (16-30), 1998
- [4] Alberts C J, Carroll C W ,Kaufman W M , Perlee C J , and Siegel M W . Automated Inspection of Aircraft, In: Technical report, no. DOT/FAA/AR-97/69, Carnegie Mellon Research Institute, Pittsburgh, PA 15230-2950, USA, 1998
- [5] Liao P. S., T. S. Chen and P. C. Chung. A Fast Algorithm for Multi Level Thresholding, In: Journal of Information Science and Engineering 17, page numbers (713-727), 2001
- [6] Lee S. U. and S. U. Chung. A Comparative Performance Study of Several Global Thresholding Techniques for Segmentation, In: Computer Vision Graphics Image Processing, Volume 52, page numbers (171-190), 1990
- [7] Tsai D. M. and Chen Y. H. A Fast Histogram Clustering Approach for Multi Level Thresholding, In: Pattern Recognition Letters, Volume 13, Number 4, page numbers (245-252), 1992
- [8] Otsu Nobuyuki. A Threshold Selection Method for Gray Level Histogram, In: IEEE Transaction on System, Man and Cybernetics, Volume SMC-9, Number 1, 1979
- [9] Kapur J. N., P. K. Sahoo and A. K. C. Wong. A New Method for Gray-level Picture Thresholding using Histogram, In: Computer Vision, Graphics and Image Processing, Volume 29, Issue 3, page numbers (273-285), 1985
- [10] Hammouda Khaled. Texture Segmentation using Gabor Filters, In: IEEE Journal "Transform", Volume 26, Issue 6, page numbers (1-8), 2000
- [11] Field D. J. Relation between the Statics of Natural Images and Response Properties of Cortical Cells, In: Journal Optical Society of America, page numbers (2379-2394), 1987
- [12] Cherng Shen. The Analysis of Osteoblast Cellular Response to the reaction of Electromagnetic Field at 2.4 GHz, In: Journal of American Science, page numbers (48-50), 2005
- [13] Ceylan M., Ceylan R., Ozbay Y. and Kara S. Application of Complex Discrete Wavelet Transform in Classification of Doppler Signals using Complex-Valued Artificial Neural network, In: Artificial Intelligence in Machines, Volume 44, Issue 1, page numbers (65-76), 2008
- [14] Do M. N. Multi Resolution Image Representation, PhD Thesis EPFL, Lausanne, Switzerland, 2001
- [15] Emmanuel J. Candes and David L. Donoho. Curvelets-A surprisingly effective non-adaptive representation for objects with Edges, In: Curve and Surface Fitting, publisher: Vanderbilt Univ. Press, Nashville, TN, 1997
- [16] Cunha A. L., Zhou J.,Do M. N. The Nonsampled Contourlet Transform: Theory, Design and Applications, In: IEEE Transaction on Image Processing, 2005
- [17] Simoncelli E. P., Freeman W. T., Adelson E. H., Heeger D. J. Shiftable Multiscale Transforms, In: IEEE Transaction on Information Theory, Volume 38, number. 2, page numbers (587-607), 1992

- [18] Mumtaz M., Mansoor Atif B. and Masood H. A New Approach to Aircraft Surface Inspection Based on Directional Energies of Texture, In: International Conference on Pattern Recognition, ISSN: 1051-4651, page numbers (4404-4407), 2010
- [19] Artificial Neural Network Available at weblink:  
[http://www.usegnu.net/projects/files/ANN\\_Project.pdf](http://www.usegnu.net/projects/files/ANN_Project.pdf)
- [20] Do M. N., Vetterli M. Contourlets In: Beyond wavelet, J. Stoeckler and G.V. Welland, Eds. Academic Press, New, 2003
- [21] Do M. N. (2003): Available at weblink: <http://www.ifp.uiuc.edu/~minhdo/software/>
- [22] Rao, Kamisetty Ramamohan and Yip, P. Discrete Cosine Transform: Algorithms, Advantages, Applications, In: Academic Press, ISBN-13: 9780125802031 ISBN: 012580203X, NV, USA, 1990